Modelling flexible multi-body systems within the Udwadia-Kalaba framework, a lumped parameter approach

E J. H. Yap[1], D. Rezgui[2], M.H. Lowenberg[3], S.A Neild[4],
University of Bristol, Bristol, BS8 1TR, United Kingdom

A.K. Rahman[5]
BAE Systems, Rochester, Kent, ME1 2XX, United Kingdom

It is common practice within Multi-Body Dynamic (MBD) modelling to assume that individual bodies are rigid however this can be an oversimplification especially when slender bodies are present resulting in inaccurate estimations of the system's natural frequencies and overall behaviour. To address this shortfall, we extend the Udwadia-Kalaba (U-K) MBD formulation in this paper to model flexible multibody systems for purposes of exploring system natural frequencies. To model the flexibility, a lumped parameter approach is proposed, which in this work idealises a flexible beam as a series of discrete rigid elements connected by torsional springs. In the U-K formulation, a mechanical system can also be discretised into rigid elements and adapted. This is viewed as a benefit for incorporating a lumped parameter approach within the U-K formulation to model flexible multibody systems. A flexible crank-slider mechanism is introduced and modelled within the Udwadia-Kalaba formulation to capture the dynamics of flexibility through linkage compliance. The model is validated against an alternatively formulated MBD model and system natural frequencies and mode shapes numerically predicted. Results of the study show the effectiveness and potential of extending the application of the Udwadia-Kalaba formulation by using a lumped parameter approach to dynamically model flexible multibody systems.

1. Introduction

The study of Multi-Body Dynamic (MBD) modelling approaches is integral to the analysis of mechanical systems that display large displacements, geometric non-linearities and feature joints which dictate the range of permittable kinematic motion of system components. With the advancements in technological developments in addition to improved understanding of compliant mechanisms and systems, modern engineering structures are increasingly designed to operate in envelopes that exceed the realms where linear based assumptions may be used. This often results in systems with components exhibiting deflections well into the nonlinear range where linear equations are no longer appropriate in defining their motions. With advantages of compliant systems including simplified manufacturing, reduced wear and elimination of lubrication [1], the projected continual growth in their applications means considerable effort and emphasis is placed on developing techniques to facilitate the design and analysis of such nonlinear systems [1].

[1] Aerospace Engineering PhD student, Department of Aerospace Engineering.
e-mail: edward.yap@bristol.ac.uk
[2] Senior Lecturer in Aerospace Engineering, Department of Aerospace Engineering
e-mail: djamel.rezgui@bristol.ac.uk
[3] Professor of Flight Dynamics, Department of Aerospace Engineering
email: m.lowenberg@bristol.ac.uk
[4] Professor in Nonlinear Structural Dynamics, Department of Mechanical Engineering
email: simon.neild@bristol.ac.uk
[5] Principal Mechanical Analysis Engineer, Electronic Systems
email: khosru.rahman@baesystems.com

Whilst methods such as nonlinear finite element analysis (FEA) and software applications including MSC Adams, Dymore and ANSYS [2-4] are readily available for the analysis of MBD systems that display nonlinear dynamic behaviour, this paper will primarily concern its discussion around analytical based approaches for modelling MBD systems. This is due to the insight that can be gained into the fundamental equations underpinning the modelling of an MBD system. The use of analytical based MBD approaches, implemented within tools such as MATLAB, is also conducive for implementing control theory to the MBD model should this be of interest to the analyst. In addition, low-cost analytical models are often desired [1] that may accurately capture system geometric nonlinearities, and provide access to the underlying model equations, whilst providing capabilities for parametric design insight. One such analytical modelling approach is the U-K formulation [5] – this is the modelling approach of primary consideration in this paper. The U-K formulation specifically address the modelling of multibody mechanical systems subjected to kinematical constraints. The formulation can be used to model a mechanical system as a system of rigid bodies, with geometrical constraint equations governing their physical kinematical motions. Previous investigations of this dynamic modelling approach [6,7,8] showed convincing agreement of simulated system dynamic results with reference data. Udwadia and Phohomsiri in [9] note that alternative analytical formulations of constrained system motion were offered by Gibbs and Appell, Gauss and Dirac, however emphasise that a key feature of the U-K formulation is that it may provide an explicit set of equations for generic constrained systems. The U-K formulation was also investigated in scenarios where constrained mechanical systems contained nonideal constraints [10] or singular mass matrices [11]. Results of these studies showed the formulation was able to handle such situations through modifications in the equations of motion, further highlighting the contribution of the U-K modelling approach for the analysis and control of multi-body systems [9]. Udwadia and Schutte furthered the work in [11] by deriving and obtaining a simpler set of equations in the form of the U-K formulation that are valid for systems exhibiting positive definite and/or singular mass matrices [12].

The U-K formulation's solution techniques can also be efficient [13] with Bauchau attributing this to the formulations resulting in a system of Ordinary Differential Equations (ODEs) which may be solved with standard explicit time integration solvers. Furthermore, the formulations have the benefit of eliminating the use of Lagrange multipliers which have often been noted to be difficult to obtain for large number degree of freedom systems [9].

Previous work of the authors [14] considered the application of the U-K modelling approach to model a nonlinear and rigid crank-slider mechanism, and nonlinear multibody aircraft inceptor system. Under the influence of an externally applied sinusoidal load, the mechanism's dynamic behaviour was assessed with results shown to match responses from alternatively formulated models. These models included a reduced coordinate Lagrangian model and a model produced within MATLAB's MBD toolkit Simscape [15]. The results of the study highlighted the applicability of the U-K modelling approach in representing the dynamics of generic multibody systems that were subjected to kinematical constraints and also displayed nonlinear behaviour.

In the aforementioned studies [6,7,8,14], the U-K formulation was applied to model rigid-body systems. Various studies have discussed and explored methodologies of applying the U-K formulation to deal with flexible systems. Examples include Antunes et al. [16-18] who demonstrated a modelling strategy for continuous flexible systems by transforming the U-K formulation into modal coordinate space. Gutiérrez and Heidecker [19] combined the assumed modes method within the U-K framework to model flexible structures by approximating the differential equation model of continuous systems. Pennestri et al. [20] assessed the numerical efficiency of the U-K formulation in analysing the dynamics of a flexible linkage against an alternative coordinate partitioning scheme through an application study of a slider-crank mechanism; as an additional element of novelty, Pennestri et al. modelled the coupler by a single Timoshenko beam element.

In this paper, the authors offer an alternative methodology to model flexible multibody systems using the U-K formulation by extending the notion of rigid body modelling through a lumped parameter approach. In the lumped parameter approach, a flexible body is discretised into a series of rigid elements with lumped masses connected by flexible joints. However in the lumped parameter approach adopted in this work, a flexible body is discretised into a series of rigid elements with lumped masses, connected by torsional springs to represent bending flexibility. In the U-K formulation, a mechanical system can be adapted to be similarly discretised into rigid elements; this was viewed as a benefit for incorporating a lumped parameter approach within the U-K formulation to model flexible multibody systems. An additional benefit is that within the U-K formulation, beam model equations may be generalised to enable a U-K formulated beam model to be automatically formulated for a chosen number of rigid elements; the fidelity that a flexible beam is discretised into may be autonomously prescribed to facilitate the rapid dynamic analysis of flexible systems to meet accuracy requirements.

Furthermore, the aspect of modelling flexible bodies contained within wider mechanisms, and capturing the resulting multibody system's flexible modes may be readily handled by this proposed modelling methodology, so long as respective geometric constraint equations are identified and appended within the U-K formulation. A case study of a flexible crank-slider mechanism is presented to demonstrate proof of concept of using a lumped parameter approach within the U-K framework to model flexible bodies integrated within wider mechanisms to capture flexible modes of the complete multibody system.

It is common practice to extend existing modelling methodologies for rigid systems when dealing with flexible multibody dynamics [21]. Previous work by the authors [22] developed a framework and demonstrated the applicability of using a lumped parameter approach within the U-K modelling framework to predict natural frequencies and mode shapes of a flexible beam. The results were validated against a beam modelled within MSC Patran [23]. Neild et al. [24] also investigated representing a beam as a series of rigid elements connected by springs and formalised a methodology in representing a beam in discrete form that also provides insight to the physical representation of the flexible beam. This methodology [24] is adopted herein to approximate the dynamics of a flexible beam contained within a larger mechanism, and to investigate implications on the mechanism's resulting natural frequencies.

The following section provides an overview outline of the Udwadia-Kalaba MBD modelling approach. Section 3 introduces the crank-slider mechanism for which the dynamics is modelled using the U-K formulation assuming rigid body dynamics. The mechanism's natural frequencies are numerically predicted and compared with frequencies obtained from conducting forced time response simulations of the U-K formulated mechanism model. Section 4 then demonstrates the adaptation of the U-K approach to modelling flexible bodies in the form of a flexible beam in discrete form. In Section 5, the presented crank-slider mechanism model is extended to consider the dynamics of flexibility. A lumped parameter representation of a beam modelled within FEA is integrated within the crank-slider mechanism model. Responses of the resulting flexible crank-slider mechanism are compared with those from an alternatively formulated model and natural frequencies numerically predicted.

2. The Udwadia-Kalaba MBD modelling approach

The Udwadia-Kalaba equations of motion specifically address the modelling of multi-body mechanical systems subjected to kinematical constraints. The underlying basis of the formulations follow the Gauss principle of least constraint which dictate that the accelerations that materialize for a system are those that minimize the Gaussian scalar quantity [5]. The U-K formulation effectively reduce a mechanical system to a corresponding system of rigid bodies with their physical kinematical motion governed by

the system's geometrical constraint equations. Hence the U-K formulation place heavy emphasis on the accurate derivation of the system's geometric constraint equations. The U-K equations [5] are

$$\ddot{\mathbf{x}} = \mathbf{a} + \boldsymbol{M}^{-\frac{1}{2}}\left(\boldsymbol{A}\boldsymbol{M}^{-\frac{1}{2}}\right)^{+}(\boldsymbol{b} - \boldsymbol{A}\mathbf{a}), \tag{1}$$

where $\ddot{\mathbf{x}}$ is the vector of true accelerations of the multibody system including the influence of applied kinematical constraints. It is of size (u x 1) where u denotes the number of system state variables. **a** refers to a vector of external accelerations resulting from impressed forces acting on the system and is of size (u x 1). It is often referred to as the accelerations of the unconstrained system. $\boldsymbol{M}$ refers to the mass matrix of the system, with size (u x u). The + symbol is the Moore-Penrose generalised inverse function [25]. The use of this inverse is what alleviates the need to consider the notion of Lagrange multipliers in the explicit equations of motion formulation for constrained multibody systems [9]. The U-K formulation assumes that the system's accelerations between rigid bodies resulting from the derived constraint equations may be expressed in the form of linear equality relations given by

$$\boldsymbol{A}\ddot{\mathbf{x}} = \boldsymbol{b}. \tag{2}$$

Here $\boldsymbol{A}$ is a (v x u) matrix associated with the system's state accelerations obtained from differentiating the system's geometric constraint equations twice with respect to time and arranged in the form of Eq. (2). The quantity v refers to the number of geometric constraint equations derived for the system. $\boldsymbol{b}$ denotes a vector of size (v x 1) populated with terms unassociated with state accelerations when the geometric constraint equations are differentiated twice with respect to time and formulated in the form of Eq. (2).

Upon closer inspection of Eq. (1), the right hand side terms constituting $\boldsymbol{M}^{-\frac{1}{2}}\left(\boldsymbol{A}\boldsymbol{M}^{-\frac{1}{2}}\right)^{+}(\boldsymbol{b} - \boldsymbol{A}\mathbf{a})$ effectively represent the additional accelerations introduced by virtue of the system constraints, to ensure that the system complies and does not deviate from its prescribed constraints for every instance of time. The accelerations of the unconstrained system **a** within Eq. (1) may be obtained from evaluating Lagrange's equation

$$\frac{d}{dt}\left(\frac{\partial L}{\partial \dot{q}_j}\right) - \frac{\partial L}{\partial q_j} + \frac{\partial R_D}{\partial \dot{q}_j} - Q_j = 0 \tag{3}$$

where q_j represents a generalised coordinate, $\dot{q}_j$ is its time derivative and subscript j refers to the generalised coordinate index. L is the Lagrangian quantity associated with the kinetic-potential energy balance of the system and R_D is an energy function term that arises due to the presence of dissipative forces within the system. Q_j represents the generalised forces acting on the system associated with the j^{th} generalised coordinate.

The caveat with using Lagrange's equation here is to treat the virtual displacements of individual generalised coordinate terms as though they are independent of one another, as though no constraints are present within the system to associate the generalised coordinates. By treating the generalised coordinates as being independent, the acceleration equations that result therefore represent those of the unconstrained system, hence **a** in Eq. (1) is obtained.

3. The crank-slider mechanism- rigid multibody dynamics

The rigid body dynamics of the crank-slider mechanism is firstly presented and discussed prior to showing how the U-K formulation may be extended using a lumped parameter approach to approximate

the dynamics of bending flexibility within the mechanism. The geometry of the crank-slider mechanism is shown in Fig. 1. It is a planar mechanism, comprising two links namely a crank link and slider link, both assumed to be rigid. The mechanism's crank link is denoted by subscript 1 whilst the slider link is denoted by subscript 2 in accordance with the notation within the illustration. One end of the crank link is attached to the ground through a revolute joint whilst one end of the slider link is attached to the ground through a translational-revolute joint to permit translational displacement. The crank and slider links are connected to one another through a revolute joint at their ungrounded ends and a spring-dashpot is attached between the two links to provide means of translational resistance and energy dissipation. The mechanism's revolute joints and translational-revolute joint are all assumed frictionless.

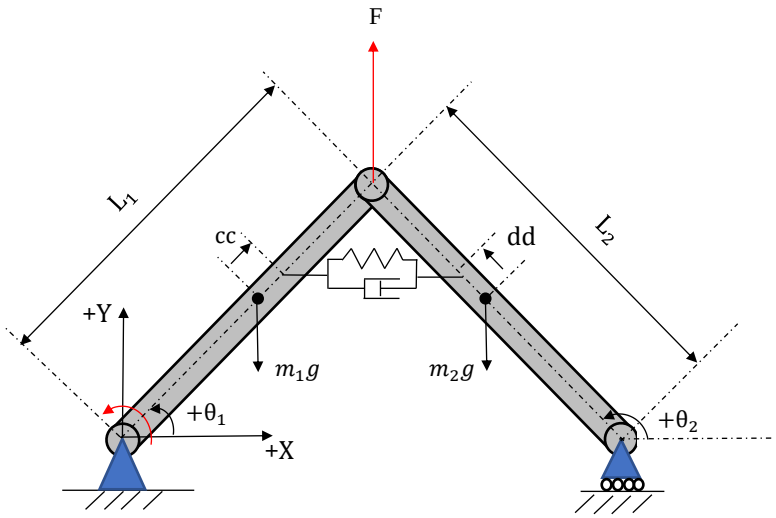

Fig. 1: Rigid crank-slider mechanism

In Fig. 1, the global axes is located at the centre of the crank link ground revolute joint, with positive translational and rotational displacements indicated. The model parameters considered for the crank-slider mechanism are presented in Table. 1.

Table. 1: Rigid crank-slider mechanism parameters

Symbol	Parameter	Value	Unit
L_1	Length of crank link	$2\sqrt{2}$	m
L_2	Length of slider link	$2\sqrt{2}$	m
m_1	Mass of crank link	1	kg
m_2	Mass of slider link	1	kg
cc	Spring-dashpot attachment offset distance from crank link centre of gravity	0	m
dd	Spring-dashpot attachment offset distance from slider link centre of gravity	0	m
$k_{\text{spring-dashpot}}$	Spring stiffness	50	Nm^{-1}
L_0	Spring equilibrium length	2	m
$c_{\text{spring-dashpot}}$	Dashpot damping coefficient	5	Nsm^{-1}

Both the mechanism's crank and slider links are equal in length and equal in mass. With the parameters cc and dd taking a null value from Table. 1, the mechanism's spring-dashpot is horizontally level and

attached to the crank and slider links at their centres of gravity (CG). In Fig. 1, F refers to an externally applied force, chosen to be applied vertically at the connection between the crank and slider link although this point of application is not limited. The acceleration due to gravity, g is a scalar value of $9.81\mathrm{ms}^{-2}$ assumed to act in the negative Y-direction.

The configuration of the crank-slider mechanism, with both links assumed rigid and their CGs at each of their respective centres, may be described by six geometrical positional states X_1, Y_1, θ_1, X_2, Y_2, θ_2. With reference to Fig. 1, subscript 1 refers to the mechanism's crank link and subscript 2 refers to the slider link. X_i and Y_i denote the link's centre of gravity translation in the global axes whilst θ_i refers to the orientation of the link relative to the horizontal. The constraint equations governing the range of kinematic motion of the mechanism due to its geometry are defined as

$$\mathrm{X}_1 - \frac{\mathrm{L}_1}{2}\cos(\theta_1) = 0 \tag{4}$$

$$\mathrm{Y}_1 - \frac{\mathrm{L}_1}{2}\sin(\theta_1) = 0 \tag{5}$$

$$\mathrm{X}_1 + \frac{\mathrm{L}_1}{2}\cos(\theta_1) - \mathrm{X}_2 - \frac{\mathrm{L}_2}{2}\cos(\theta_2) = 0 \tag{6}$$

$$\mathrm{Y}_1 + \frac{\mathrm{L}_1}{2}\sin(\theta_1) - \mathrm{Y}_2 - \frac{\mathrm{L}_2}{2}\sin(\theta_2) = 0 \tag{7}$$

$$\mathrm{Y}_2 - \frac{\mathrm{L}_2}{2}\sin(\theta_2) = 0 \tag{8}$$

3.1 The crank-slider mechanism- rigid dynamic response

To model the mechanism's dynamic response using the U-K formulation, the mechanism's constraint equations are differentiated twice with respect to time to yield a set of acceleration-level constraint equations. Through rearrangement, the mechanism's accelerations due to the constraints are expressed as a linear equality relation in the format of Eq. (2) from which the $\boldsymbol{A}$ and $\boldsymbol{b}$ quantities to be used within the U-K formulation are obtained.

$$\boldsymbol{A} = \begin{bmatrix} 1 & 0 & \frac{\mathrm{L}_1}{2}\sin(\theta_1) & 0 & 0 & 0 \\ 0 & 1 & -\frac{\mathrm{L}_1}{2}\cos(\theta_1) & 0 & 0 & 0 \\ -1 & 0 & \frac{\mathrm{L}_1}{2}\sin(\theta_1) & 1 & 0 & -\frac{\mathrm{L}_2}{2}\sin(\theta_2) \\ 0 & -1 & -\frac{\mathrm{L}_1}{2}\cos(\theta_1) & 0 & 1 & \frac{\mathrm{L}_2}{2}\cos(\theta_2) \\ 0 & 0 & 0 & 0 & 1 & -\frac{\mathrm{L}_2}{2}\cos(\theta_2) \end{bmatrix} \tag{10}$$

$$\boldsymbol{b} = \begin{bmatrix} -\frac{\mathrm{L}_1}{2}\dot{\theta}_1^2\cos(\theta_1) \\ -\frac{\mathrm{L}_1}{2}\dot{\theta}_1^2\sin(\theta_1) \\ -\frac{\mathrm{L}_1}{2}\dot{\theta}_1^2\cos(\theta_1) + \frac{\mathrm{L}_2}{2}\dot{\theta}_2^2\cos(\theta_2) \\ -\frac{\mathrm{L}_1}{2}\dot{\theta}_1^2\sin(\theta_1) + \frac{\mathrm{L}_2}{2}\dot{\theta}_2^2\sin(\theta_2) \\ -\frac{\mathrm{L}_2}{2}\dot{\theta}_2^2\sin(\theta_2) \end{bmatrix} \tag{11}$$

The mechanism's unconstrained acceleration vector **a** is shown in Eq. (12) and the mass matrix $\boldsymbol{M}$ of the mechanism shown in Eq. (13). The mass matrix was prescribed and inferred directly from the mechanism's unconstrained acceleration vector.

$$\mathbf{a} = \begin{bmatrix} \frac{-k_{\text{spring-dashpot}}\frac{(2\mathrm{L}_0 + 2\mathrm{X}_1 - 2\mathrm{X}_2)}{2} - c_{\text{spring-dashpot}}\frac{(2\dot{\mathrm{X}}_1 - 2\dot{\mathrm{X}}_2)}{2}}{m_1} \\ \frac{\mathrm{F} - m_1 g}{m_1} \\ \frac{\mathrm{F}\left(\frac{\mathrm{L}_1}{2}\cos(\theta_1)\right)}{I_{\mathrm{M}_1}} \\ \frac{k_{\text{spring-dashpot}}\frac{(2\mathrm{L}_0 + 2\mathrm{X}_1 - 2\mathrm{X}_2)}{2} + c_{\text{spring-dashpot}}\frac{(2\dot{\mathrm{X}}_1 - 2\dot{\mathrm{X}}_2)}{2}}{m_1} \\ \frac{-m_2 g}{m_2} \\ 0 \end{bmatrix} \tag{12}$$

$$\boldsymbol{M} = \begin{bmatrix} m_1 & 0 & 0 & 0 & 0 & 0 \\ 0 & m_1 & 0 & 0 & 0 & 0 \\ 0 & 0 & I_{\mathrm{M}_1} & 0 & 0 & 0 \\ 0 & 0 & 0 & m_2 & 0 & 0 \\ 0 & 0 & 0 & 0 & m_2 & 0 \\ 0 & 0 & 0 & 0 & 0 & I_{\mathrm{M}_2} \end{bmatrix} \tag{13}$$

In Eq. (12), I_{M_i} is the mass moment of inertias of the mechanism's i^{th} link, taken about its respective centre of gravity in the axis about which the links rotate. In Eq. (12), the virtual displacements corresponding to the mechanism's identified generalised coordinates were treated as being independent

of one another. The acceleration contributions due to gravity (g) and accelerations resulting from the applied externally force (F) applied vertically at the mechanism's link connections are all considered here.

Time history simulations of the U-K formulated mechanism model were conducted within MATLAB and compared against alternatively formulated models of the mechanism produced within Simscape and a minimal coordinate Lagrangian model to provide means of validation. The Simscape mechanism model, shown in Fig. 2, provides an alternative visualisation of the mechanism and respective connections. The Simscape crank-slider mechanism model is now briefly discussed, upon which the minimal Lagrangian model is addressed.

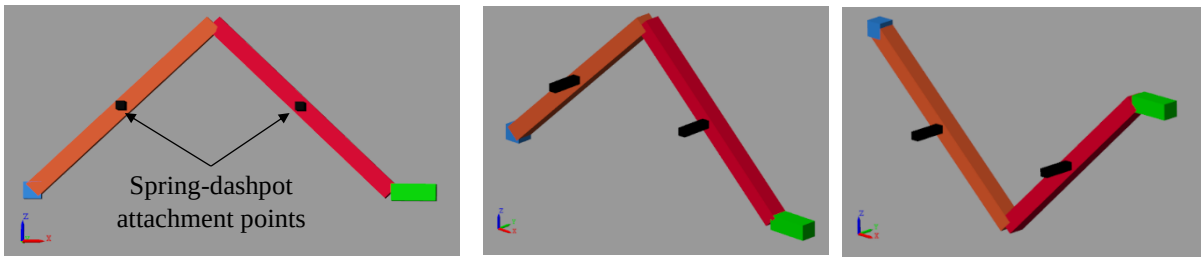

a) b) c)

Fig. 2: MATLAB Simscape model of the rigid crank-slider mechanism

The orange and red blocks in Fig. 2 represent the mechanism's crank and slider link whilst the blue block represents the crank link's ground attachment point and location of the ground revolute joint. The green block is a fictitious slider block, included as a visual aid to illustrate and emphasise the slider link's ground attachment translational-revolute joint. The black bars that project out of the crank and slider links are also fictitious blocks that were included purely as a visual aid to highlight the location of the mechanism's spring-dashpot attachment points along the centre lines of the crank and slider link. The spring-dashpot is modelled within the Simscape environment through a prismatic joint which permits translational displacement along only a single axis. The translational stiffness and damping coefficient of the prismatic joint are specified with the parameters outlined in Table. 1.

A brief overview of the processes involved within a Simscape simulation is now discussed, according to the documentation outlined in [26]. The process Simscape adopts in simulating a model involves firstly constructing a system of equations to solve for the physical network created by the connection of user-specified block ports [26]. Initial conditions that satisfy the model's equations are then solved, for all system variables contained within the Simscape model before the simulation is initiated. The simulation comprises two primary phases: a transient initialisation phase and transient solve phase. In the initialisation phase, all dynamic variables within the Simscape model are fixed by the Simscape solver whilst algebraic variables and dynamic variable derivatives are solved to obtain a set of consistent initial conditions for system variables which are then passed into the solve phase. In the solve phase, the system's continuous differential equations are integrated in the time domain until an event occurs such as a discontinuity or a zero crossing, where a mathematical function changes sign. If either event is encountered, the initialization phase of the simulation is returned to by the Simscape solver and initial conditions for system variables re-determined and passed back into the solve phase – this cycle repeats until the simulation completes.

To illustrate the concept of a network of block connection ports within the Simscape modelling environment, a block schematic of the Simscape rigid crank-slider mechanism model is shown in Fig. 3.

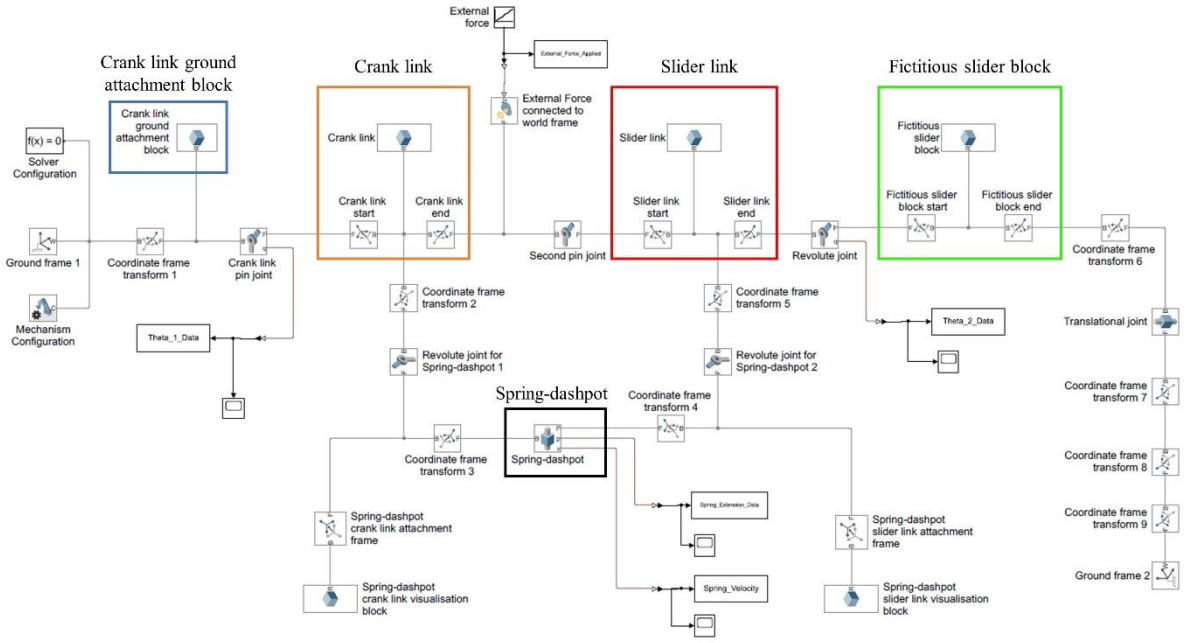

Fig. 3: Simscape crank-slider mechanism model block schematic

In Fig. 3, the blocks and corresponding connections associated with the mechanism's crank and slider links are highlighted in the orange and red groupings. The mechanism's crank link ground attachment point is represented by the block highlighted in the blue outline and the mechanism's fictitious slider block and spring-dashpot are also highlighted. The mechanism's crank link, slider link and fictitious slider block in Fig. 3 were constructed by firstly inserting a solid block where block dimensions and dynamic properties are specified. However, to recognise their physical rigid nature within the Simscape modelling environment, two rigid frame transforms were prescribed for each solid block as shown in Fig. 3, that originate from the block's centre of gravity and project outwards to define the block's physical fore and aft edge boundaries where additional model network port connections may attach to.

The basis of the minimal coordinate Lagrangian model is to use a single generalised coordinate to fully express the mechanism's equation of motion within Lagrange's equation. By inspecting Eq. (4)-(8), the mechanism's constraint equations, six geometrical positional states are associated through five constraint equations; the mechanism is an effective a single degree of freedom system and can be fully described by the generalised coordinate θ_1 alone.

A sample of dynamic time history simulation responses of the U-K rigid crank-slider mechanism model are presented in Fig. 4 and compared against the alternatively formulated Simscape and minimal coordinate Lagrangian models, to provide a means to validate the U-K formulated mechanism model. The U-K mechanism model was solved within MATLAB using the standard ode15s solver with specified relative tolerance of 1e-6 and absolute tolerance of 1e-8.

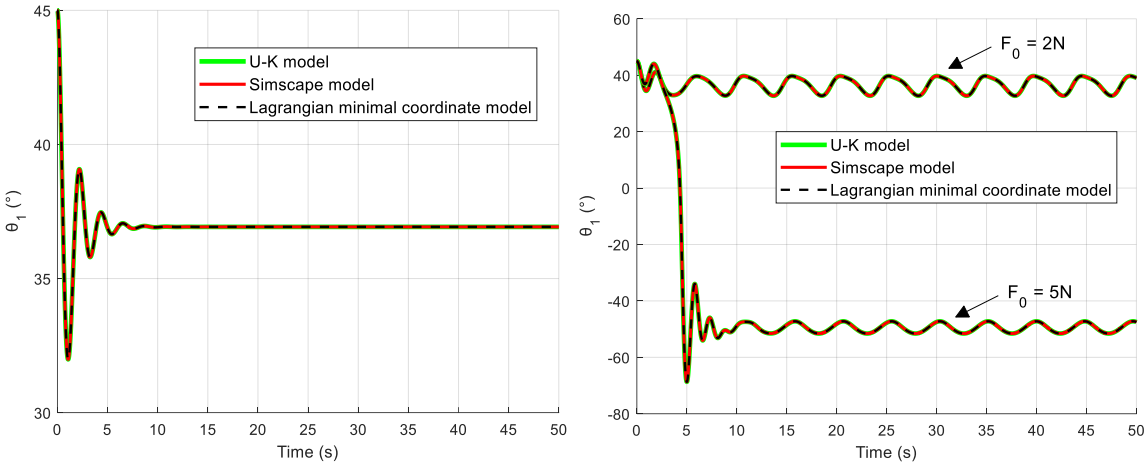

a) b)

Fig. 4: Rigid crank-slider mechanism (a) free response under gravity, (b) forced response under the application of external sinusoidal loads and gravity (forcing amplitudes F_0 = 2N, 5N. Forcing frequency, ω: 1.3rads^{-1}).

In Fig. 4 the quantity displayed is the orientation of the mechanism's crank link to the horizontal, θ_1, as defined in Fig. 1. The time history simulations were conducted with θ_1 initially orientated at 45°. In the forced response time history simulations in Fig. 4(b), two vertical sinusoidal forces with forcing amplitudes 2N and 5N were applied at the mechanism's crank-slider link connection. The associated forcing frequency for both loading cases was 1.3rads^{-1}. Fig. 4(b) reveals the bistable nature of the mechanism, with responses attracted to either 'lower' ($\theta_1 < 0$) or 'upper' ($\theta_1 > 0$) limit cycle solutions depending upon the forcing amplitude level applied. The responses from the U-K formulated model in Fig. 4 show a direct match with dynamic time history responses produced from both the Simscape and minimal coordinate Lagrangian models. This validates the implementation of the U-K formulation whilst also demonstrating the generic applicability and simplicity of the U-K formulation to model constrained multibody systems that also exhibit nonlinear behaviour.

The U-K formulation results in a system of ODEs that provide direct access to the linearised system's Jacobian matrix from which system modal properties such as natural frequencies and mode shapes may be numerically evaluated. For the rigid crank-slider mechanism defined with parameters in Table. 1, its modal frequencies and corresponding mode shapes were numerically obtained from evaluating the eigenvalues of the linearised system's Jacobian matrix at equilibrium conditions – which for simplicity was specified in the absence of gravitational forces, external forcing, and with the crank link θ_1 orientated at 45° from the horizontal so as to equilibrate the mechanism's spring. A single modal frequency was numerically predicted at 0.616Hz. For validation, the Simscape mechanism model's natural frequencies were numerically extracted by defining open loop linearisation input and output points within in the model's physical signal network. A single frequency was numerically predicted at 0.616Hz. The agreement of natural frequencies numerically predicted from the U-K and Simscape models provides confidence and validation in the method of evaluating a linearised system's Jacobian matrix within the U-K formulation, to extract its modal properties.

To further assess the U-K model in terms of predicting the mechanism's natural frequency, forced response time history simulations of increasing forcing amplitudes and frequency levels were conducted on the U-K mechanism model to emulate a frequency response (FR) analysis as seen in Fig. 5. The forced time history simulations were conducted in the absence of gravity to be consistent with the conditions that were used to numerically obtain the U-K mechanism model's modal frequency.

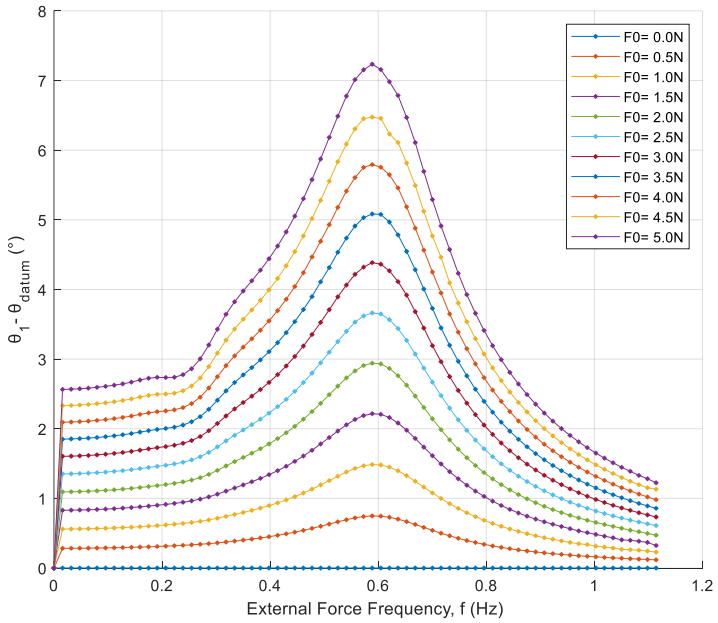

Fig. 5: U-K formulated rigid crank-slider mechanism model frequency responses

Individual frequency response plots in Fig. 5 were obtained from conducting forced time history simulations with an external sinusoidal excitation load applied vertically at the connection between the mechanism's crank and slider link. The amplitude of this externally applied sinusoidal load was incremented by 0.5N for every successive time history simulation run. Additionally, for each forcing amplitude run considered, frequency sweeps were conducted in step intervals of $0.1 rads^{-1}$ between the range 0 and $7 rads^{-1}$, corresponding to an upper limit of approximately 1.1Hz in Fig. 5. At each forcing frequency level, the response was continued until the transient had subsided, resulting in an oscillation of constant amplitude; the maxima of solutions were extracted for FR analysis before the forcing frequency level was incremented. The FRs in Fig. 5 further highlight the nonlinear nature of the crank-slider mechanism through the presence of a mild softening effect with individual resonance peak locations shown to subtly reduce with increasing externally applied forcing amplitudes. This demonstrates the capability of the U-K modelling approach to capture nonlinearities within a system. Hence, where the aspect of a system's nonlinearity is of interest, the U-K formulation has shown to be a suitable modelling approach that can assess both the system's linear and nonlinear dynamic characteristics such as natural frequencies.

Results of the frequency response analysis performed on the U-K crank-slider mechanism model in Fig. 5 indicate the presence of a modal frequency in the region of 0.6Hz. This observation aligns well with the mechanism's linearised natural frequency numerically evaluated at 0.616Hz and provides further confidence in the method of evaluating a linearised system's Jacobian matrix within the U-K formulation to extract its modal properties.

This methodology will be adopted in the remainder of this paper as the primary means for extracting the modal properties of a system modelled within the U-K formulation. Concluding the discussion

regarding rigid-body dynamics of the crank-slider mechanism, the U-K modelling framework is now carried forward and extended to consider modelling flexible bodies.

4. Modelling flexible systems within the U-K formulation - a flexible beam

In the extension of the U-K formulation to consider flexible multi-body systems, a lumped parameter approach based on the methodology proposed by Neild et al. [24] in representing a uniform planar beam in discrete form is adopted. The methodology idealises a uniform beam as a series of rigid elements, connected by torsional and linear springs to approximate the beam's bending and shear deformation respectively, in a manner such that the rigid elements at either end are half of the length of the remaining elements, as illustrated in Fig. 6. However, in the proceeding discussion, only the bending aspect of their discretised beam model represented by torsional springs is considered due to the primary interest in modelling a flexible system's bending flexibility.

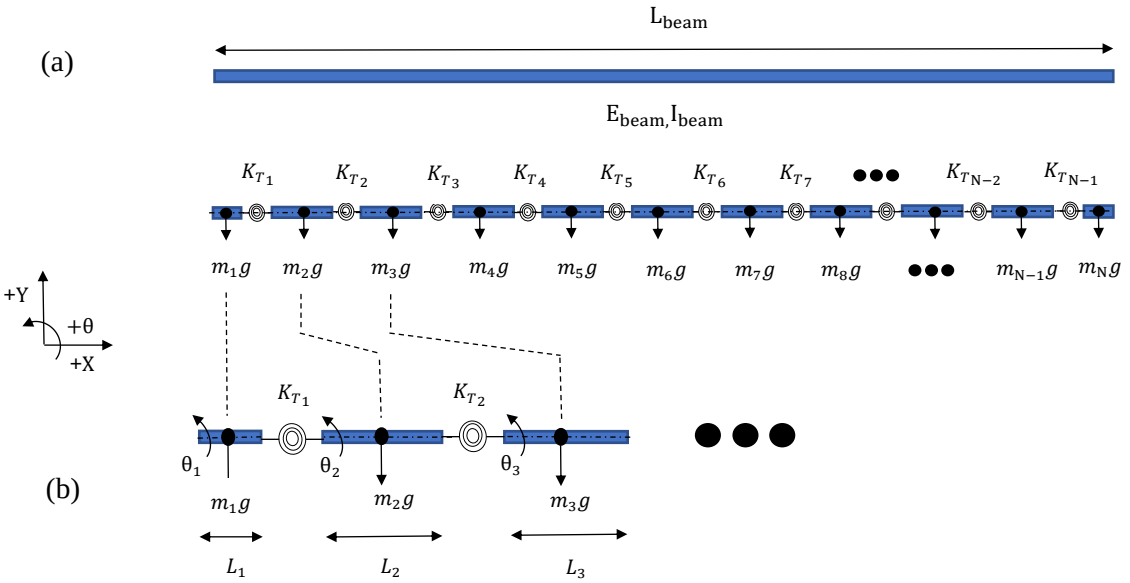

Fig. 6: (a) Original beam (b) lumped parameter diagrammatic view of the original beam

In Fig. 6(a), L, E and I represent the length, elastic modulus and second moment of area of the original flexible beam. The second moment of area is taken about the axis of rotation concentric with the beam's centre of gravity. In Fig. 6(b), the lumped parameter model of the flexible beam, m_i denotes the mass of individual rigid elements, K_{T_i} denotes the stiffness of individual torsional springs and L_i the length of individual rigid elements. The subscript N denotes the number of rigid elements the beam is discretised into. The length of each rigid element is prescribed as $\mathrm{L_{beam}}/(\mathrm{N}-1)$ whilst the first and last elements have their lengths defined by $\left(\frac{L_{beam}}{\mathrm{N}-1}\right)/2$. In similar fashion, the mass of each rigid element is given by $\mathrm{M_{beam}}/(\mathrm{N}-1)$ with the exception of the first and last elements which have mass prescribed by $\left(\frac{\mathrm{M_{beam}}}{\mathrm{N}-1}\right)/2$. $\mathrm{M_{beam}}$ refers to the total mass of the uniform flexible beam and θ_i represents the orientation of the rigid element to the global horizontal.

The centre of gravity of individual rigid elements are assumed to lie at their centres and so within the Udwadia-Kalaba formulation, the constraint equations governing the individual rigid element's centre

of gravity translation in the global frame of reference, in accordance with the notation defined in Fig. 6(b), can be simply written as:

$$\mathrm{X}_2 - \mathrm{X}_1 - \frac{L_1}{2}\cos(\theta_1) - \frac{L_2}{2}\cos(\theta_2) = 0 \tag{14}$$

$$\mathrm{Y}_2 - \mathrm{Y}_1 - \frac{L_1}{2}\sin(\theta_1) - \frac{L_2}{2}\sin(\theta_2) = 0 \tag{15}$$

$$\vdots$$

$$\mathrm{X}_\mathrm{N} - \mathrm{X}_{\mathrm{N}-1} - \frac{L_{\mathrm{N}-1}}{2}\cos(\theta_{\mathrm{N}-1}) - \frac{L_\mathrm{N}}{2}\cos(\theta_\mathrm{N}) = 0 \tag{16}$$

$$\mathrm{Y}_\mathrm{N} - \mathrm{Y}_{\mathrm{N}-1} - \frac{L_{\mathrm{N}-1}}{2}\sin(\theta_{\mathrm{N}-1}) - \frac{L_\mathrm{N}}{2}\sin(\theta_\mathrm{N}) = 0 \tag{17}$$

This lumped parameter methodology may be readily transferred to consider non-uniform beam members as the mass distribution and length of the defined rigid elements may be non-uniform. In particular, this lumped parameter method also provides insight to the physical representation of the original flexible beam. With the uniform flexible beam discretised as in Fig. 6(a), the theoretical expression for the stiffness of individual torsional springs from static loading conditions may be prescribed [24], as:

$$K_{T_i} = \frac{E_i I_i}{l_i} \tag{18}$$

In Eq. (18), E_i and I_i are the Young's Modulus and second moment of area of the original flexible beam at the location of the i^{th} torsional spring. l_i is defined as the length between the centre of gravity of rigid element i to the centre of gravity of rigid element $i+1$, and effectively represents the portion of the original beam's compliance that is accounted for by torsional spring K_{T_i} in the beam lumped parameter model. This is with the exception of the end rigid elements in which case l_1 and $l_{\mathrm{N}-1}$ refer to the length from the end rigid element free edge to the centre of gravity of the adjacent rigid element, as in Fig. 7.

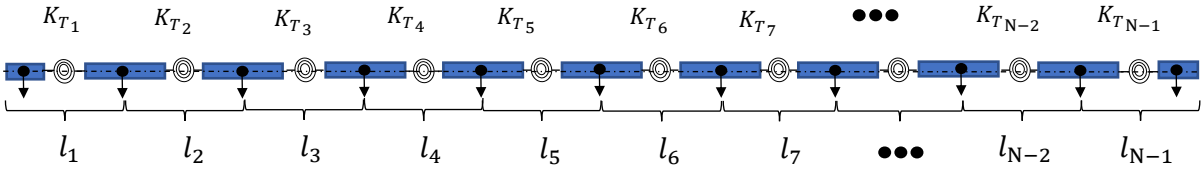

Fig. 7: Beam distributed compliance across length segments l

From Fig. 7, discretising a uniform beam using this lumped parameter method results in a uniform value for l across the entirety of the beam length, which would result in a uniform set of torsional spring stiffnesses K_{T_i}, as obtained from Eq. (18). However, this is not necessarily the case especially when considering non-uniform beams where the individual length of rigid elements l may be varying. To

numerically determine an adequate number of rigid elements to discretise a flexible beam into and to find the corresponding uniform torsional spring stiffness values within the U-K lumped parameter beam model, a simple iterative process was conducted. This process involved systematically incorporating uniform sets of torsional spring stiffness values and numerically evaluating the resulting U-K beam model natural frequencies (as detailed in section 3.1) until it results in a sufficient match with reference beam natural frequency values, and theoretically expected torsional spring stiffnesses obtained from Eq. (18). The reference beam natural frequencies are provided from a finite element (FE) beam model produced within MSC Patran. The FE modelled beam is planar with free-free boundary conditions and a rectangular cross section. Beam properties are tabulated below in Table. 2. This FE beam model is regarded as a true representation of the beam, referred to below as the 'original beam'.

Table. 2: Geometrical and material properties of the FE model beam

Parameter	Value	Unit
Length	$2\sqrt{2}$	m
Width	0.050	m
Height	0.0026	m
Elastic Modulus	70	GPa
Density	2710	kgm^{-3}
Poisson ratio	0.3	

In the absence of boundary conditions, the U-K lumped parameter beam model was discretised initially into three rigid elements. The number of elements was then increased to 5,9 and 20, and the influence on obtained torsional spring stiffnesses was investigated.

Table. 3: Comparison of obtained and theoretical torsional spring stiffnesses

No. rigid elements	Theoretical spring stiffness ($\mathbf{Nmrad^{-1}}$)	U-K beam model spring stiffness ($\mathbf{Nmrad^{-1}}$)	Percentage difference
3	3.6637	2.9849	18.53%
5	7.3274	7.3303	0.04%
9	14.655	14.657	0.01%
20	34.805	34.806	2.87×10^{-3} %

Results from Table. 3 show that as the flexible beam is discretised with increasing number of rigid elements, the matching and agreement between numerically obtained torsional spring stiffnesses and those theoretically obtained from using Eq. (18) significantly improve. This provides confidence in using Eq. (18) to approximate the U-K lumped parameter beam model torsional spring stiffnesses so long as a sufficient number of rigid elements are used to represent the original beam. To obtain the numerical torsional spring stiffnesses, a heuristic approach was used that involved systematically incrementing uniform values of spring stiffnesses within the U-K lumped parameter beam model until an adequate match in the beam's first natural frequency is observed with that of the original beam provided by the FE model as shown in Table. 4

Table. 4: Comparison of U-K beam model natural frequencies (NFs) for varying number of elements

Mode No.	FE beam model frequencies, Hz	3 element U-K beam model NFs, Hz	5 element U-K beam model NFs, Hz	9 element U-K beam model NFs, Hz	20 element U-K beam model NFs, Hz
1	1.704	1.704	1.704	1.704	1.704
2	4.697	2.880	4.693	4.695	4.697
3	9.208		10.15	9.190	9.207
4	15.22		11.28	15.12	15.22
5	22.74			22.24	22.73
6	31.76			29.63	31.73
7	42.28			43.08	42.20
8	54.30			43.37	54.12
9	67.83				67.44
10	82.86				82.07

In the case whereby the beam is discretised into 20 rigid elements, the extent of disparities between the numerically obtained and theoretical spring stiffness values in Table. 3 may be considered negligible. The corresponding U-K beam model frequencies from using the numerically obtained torsional spring stiffness values is also found to strongly match the original beam frequencies provided by the FE model, at least for the first ten modes as shown in Table. 4 and visualised in Fig. 8. In contrast, discretising the original beam using the minimum number of rigid elements considered (3 rigid elements) yielded the highest discrepancy of 18.5% between the numerically obtained and theoretical spring stiffness values as in Table 4.14. Using the numerically obtained spring stiffness values also resulted in an equally poor match in the U-K beam model's natural frequencies with those of the FE model; the highest discrepancy of 38.68% was recorded as shown in Fig. 8.

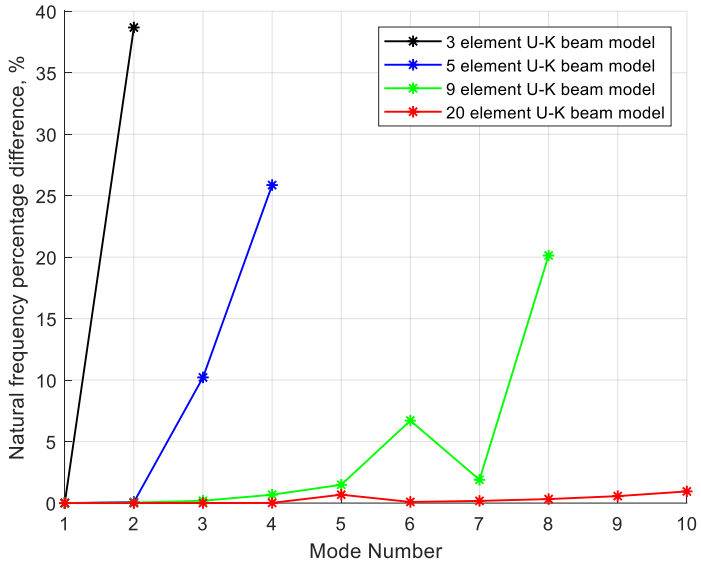

Fig. 8: Percentage differences of U-K beam model natural frequencies with those of the original beam

From Table. 4 and Fig. 8, increasing the number of rigid elements the flexible beam is discretised into notably improves the matching of the U-K beam model's modal frequencies with those of the original beam. The onset of considerable modal frequency discrepancies may be delayed to higher modes. Increasing the number of rigid elements the flexible beam is discretised by also improves the matching between the numerically obtained and theoretical torsional spring stiffness values as shown in Table. 3. These observations validate and provide confidence in using Eq. (18) to approximate the torsional spring stiffnesses within the U-K lumped parameter beam model, as long as a sufficient number of rigid elements are considered. As the number of rigid elements representing the original beam increases, the representativeness of the U-K lumped parameter beam model in capturing the dynamic characteristics of the original beam namely natural frequencies substantially improves.

The U-K beam model equations were generalised to accept any specified number of rigid elements, enabling the U-K beam model to be automatically formulated for the chosen number of rigid elements in Table. 4. This highlights a benefit of implementing a lumped parameter approach within the U-K formulation to model a system's flexibility since a mechanical system can be discretised into rigid elements, and adapted within the U-K formulation by extending the notion of rigid body modelling. This is conducive to the autonomous formulation of a flexible beam model as the number of rigid elements may be selected to facilitate rapid dynamic analysis of flexible systems to meet varying modal analysis accuracy requirements.

The results in Table. 4 and Fig. 8 provide confidence in the discretisation method of a flexible beam into rigid elements as adapted by Neild et al. in [24], as long as a sufficient number of rigid elements are used to represent the original flexible beam to hold the assumed approximations.

The extension of the U-K formulation to model a flexible body using the proposed lumped parameter approach in this section showed to be an effective framework for modelling the dynamics of flexibility of a beam, and may be readily transferred to consider non-uniform beam members. In the following section, the aspect of modelling a flexible body contained within a wider system to capture flexible modes of the multibody system is demonstrated, and will be shown to be readily handled using this lumped parameter approach methodology implemented within the U-K formulation.

5. The flexible crank-slider mechanism- flexible multibody dynamics

The dynamics of flexibility is now considered for the original crank-slider mechanism presented in Section 3. The crank link is now assumed to be deformable due to inherent flexibility as shown in Fig. 9(a), with properties of the flexible beam previously specified in Table. 2. The 20 rigid element U-K beam model from the previous section is used here to represent the flexibility of the crank link: this is justified from the results in Tables. 3 and 4 where with a 20 rigid element beam model, strong agreements were observed in obtained torsional spring stiffnesses and modal frequencies with reference theoretical values. The values of the individual torsional spring stiffnesses within the 20-rigid element lumped parameter beam model is $34.806\mathrm{Nmrad}^{-1}$, in accordance with the value obtained in Table. 3.

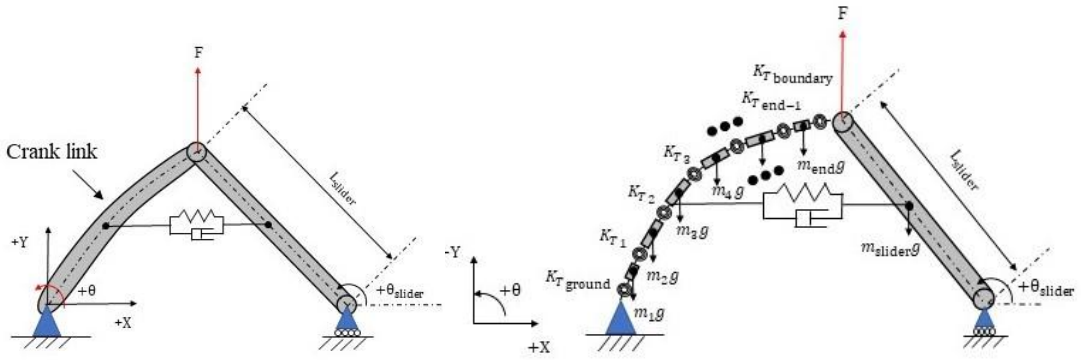

(a) (b)

Fig. 9: (a) Crank-slider mechanism with flexible crank link, (b) lumped parameter idealisation of the flexible crank link as a series of rigid elements connected by torsional springs

In Fig. 9(b), the flexible crank link is shown to be represented by six rigid elements for ease of illustration. The mechanism's slider link is treated as a rigid body with its centre of gravity defined at its centre as in Fig. 9(b). By treating the mechanism's slider link as a rigid body, the respective geometric constraint equations defining its centre of gravity translations were derived and appended into the system of constraint equations describing the lumped parameter model of the flexible crank link. In total 43 constraint equations were derived to describe the flexible crank-slider mechanism, summarised in Eq. (19). The first 40 equations describe the $\mathrm{X}_i, \mathrm{Y}_i$ centre of gravity translations of the 20 rigid elements of the crank link lumped parameter model. The remaining three constraint equations, the final three equations in Eq. (19), describe the $\mathrm{X}_i, \mathrm{Y}_i$ centre of gravity translations of the rigid slider link.

$$\left.\begin{aligned}
\mathrm{X}_1 - \frac{L_1}{2}\cos(\theta_1) &= 0 \\
\mathrm{Y}_1 - \frac{L_1}{2}\sin(\theta_1) &= 0 \\
\mathrm{X}_2 - \mathrm{X}_1 - \frac{L_1}{2}\cos(\theta_1) - \frac{L_2}{2}\cos(\theta_2) &= 0 \\
\mathrm{Y}_2 - \mathrm{Y}_1 - \frac{L_1}{2}\sin(\theta_1) - \frac{L_2}{2}\sin(\theta_2) &= 0 \\
&\vdots \\
\mathrm{X}_{\mathrm{slider}} - \mathrm{X}_{20} - \frac{L_{20}}{2}\cos(\theta_{20}) + \frac{L_{\mathrm{slider}}}{2}\cos(\theta_{\mathrm{slider}}) &= 0 \\
\mathrm{Y}_{\mathrm{slider}} - \mathrm{Y}_{20} - \frac{L_{20}}{2}\sin(\theta_{20}) + \frac{L_{\mathrm{slider}}}{2}\sin(\theta_{\mathrm{slider}}) &= 0 \\
\mathrm{Y}_{\mathrm{slider}} - \frac{L_{\mathrm{slider}}}{2}\sin(\theta_{\mathrm{slider}}) &= 0
\end{aligned}\right\} \quad (19)$$

In Eq. (19) the numbered subscripts denote the index of rigid elements within the mechanism's flexible crank link lumped parameter model and the slider subscript denotes the mechanism's rigid slider link. The length of the slider link is still taken as $2\sqrt{2}$m previously defined in Table. 2. The constraint equations in Eq. (19) were differentiated twice with respect to time and the respective vectors and matrices associated with modelling the mechanism within the U-K formulation derived as per the processes outlined in section 2. With 43 constraints and 63 geometrical positional states, the derived $\boldsymbol{A}$ matrix is of size (43 x 63) whilst $\boldsymbol{b}$ is a (43 x 1) vector. The mass matrix $\boldsymbol{M}$ is of size (63 x 63) and the unconstrained acceleration vector $\boldsymbol{a}$ of size (63 x 1); the mechanism is an effective 20 degree of freedom system.

Dynamic time history simulations were performed on the U-K formulated flexible crank-slider mechanism model and responses compared with those from an alternatively formulated model produced within Simscape for validation, shown in Fig. 10 and 11.

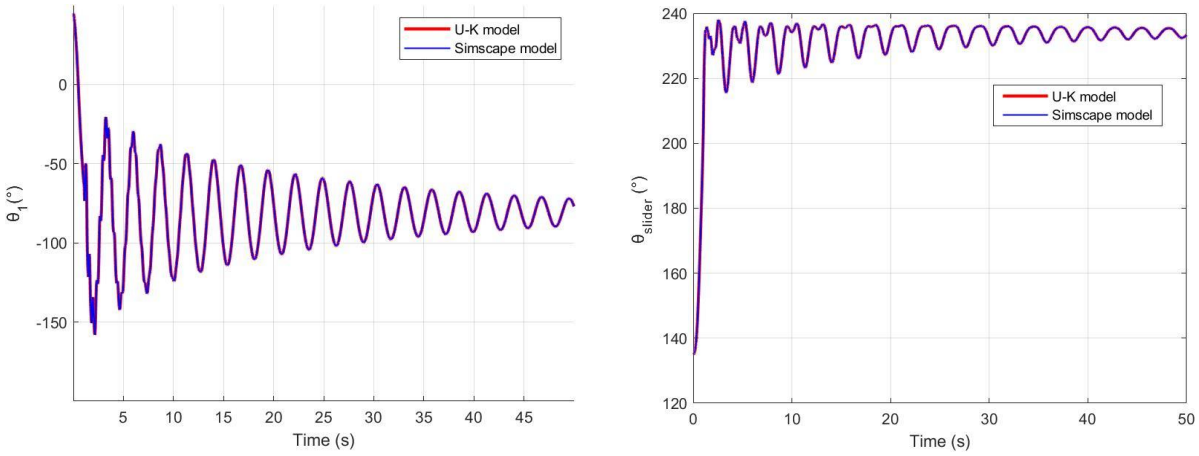

(a) (b)

Fig. 10: Flexible crank-slider mechanism free responses under gravity (a) θ_1 , (b) θ_{slider}

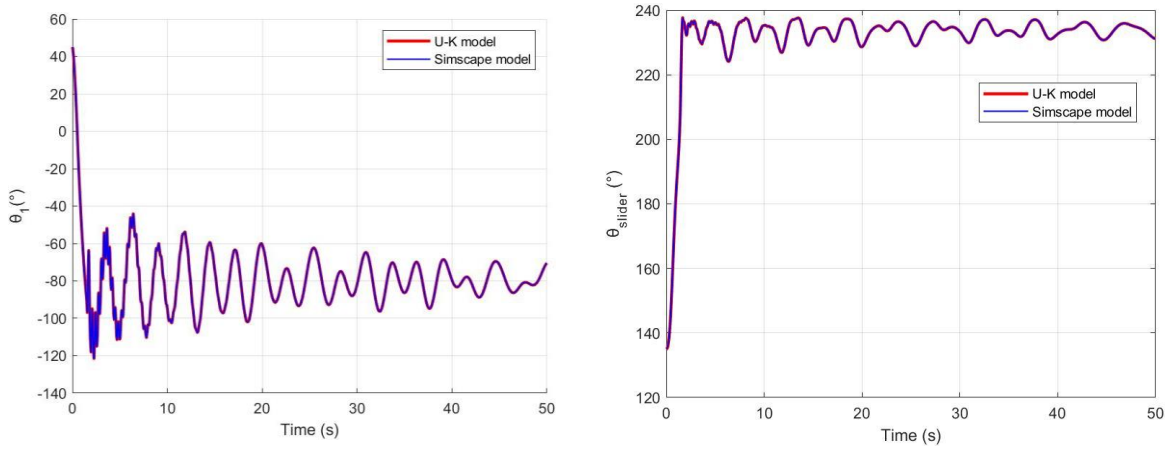

(a) (b)

Fig. 11: Flexible crank-slider mechanism forced responses under the application of external sinusoidal load and gravity (a) θ_1 , (b) θ_{slider}. External sinusoidal load applied (forcing amplitude F_0 = 5N forcing frequency, ω: 1.3 rads^{-1})

In Figs. 10 and 11, the dynamic time history responses between the U-K and Simscape flexible crank-slider mechanism models strongly match, validating the flexible crank-slider mechanism's modelling within the U-K formulation. Both the U-K and Simscape models were numerically solved using the standard MATLAB ode15s solver with a specified relative tolerance of 1e-8 and absolute tolerance of 1e-10. These tolerance values were selected as they could further converge the already strong matching responses between the U-K and Simscape models, without significantly compromising computational efficiency. The quantities displayed in Figures Figs. 10 and 11 are θ_1 and θ_{slider}, which refer to the orientation of the first rigid element within the flexible crank link lumped parameter model relative to the horizontal, and the orientation of the mechanism's rigid slider link to the horizontal. For the forced response case, an external sinusoidal force was applied vertically at the connection between the flexible crank link and rigid slider link as illustrated in Fig. 9. The forcing amplitude specified was arbitrarily chosen to be 5N, with a forcing frequency of 1.3rads^{-1} .

In the cases presented, torsional damping of value 0.05Nsmrad^{-1} was applied at the locations of individual torsional springs within the crank link lumped parameter model, to dissipate the presence of the mixed-mode responses, notably apparent within the first 10 seconds of the time simulations in Figs. 10 and 11.

The mechanism's natural frequencies and mode shapes were numerically extracted through evaluating the Jacobian matrix of the U-K formulated model to explore the mechanism's dynamic characteristics now with the inclusion of linkage flexibility. For conciseness, the mechanism's first 10 modal frequencies and corresponding mode shapes are shown below. The modal frequencies are presented in Table. 5, alongside those evaluated from the Simscape model for validation.

Table. 5: Flexible crank-slider mechanism modal frequencies

Mode	**U-K model frequencies, Hz**	**Simscape model frequencies, Hz**
1	0.285	0.285
2	1.73	1.73
3	3.06	3.06
4	6.83	6.83
5	12.1	12.1
6	18.8	18.8
7	27.1	27.1
8	36.8	36.8
9	48.0	48.0
10	60.6	60.6

The mechanism's corresponding mode shapes are presented across Figs. 12 and 13. In the plots, the X-Y displacements of individual rigid element CGs within the mechanism are plotted, including that for the rigid slider link, hence the appearance of the furthermost X-displacement point position in the mode shape plots.

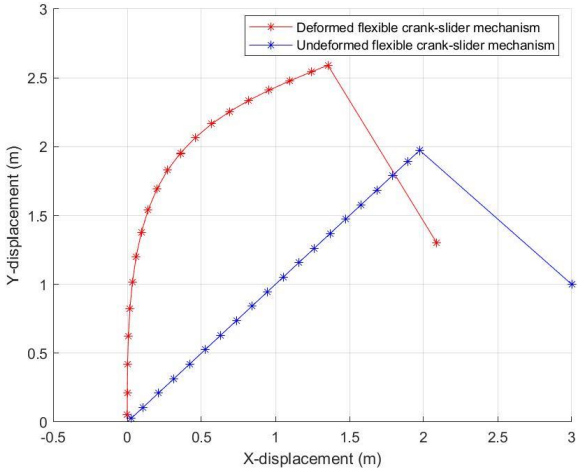

Mode 1 at 0.285Hz

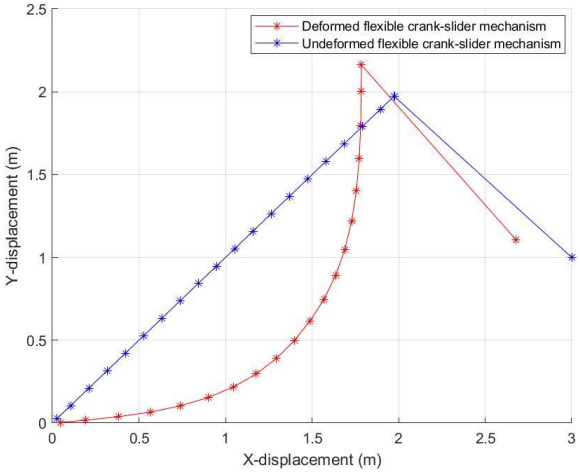

Mode 2 at 1.73Hz

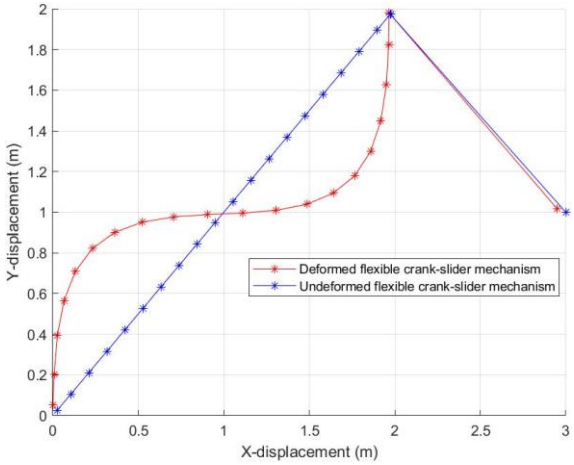

Mode 3 at 3.06Hz

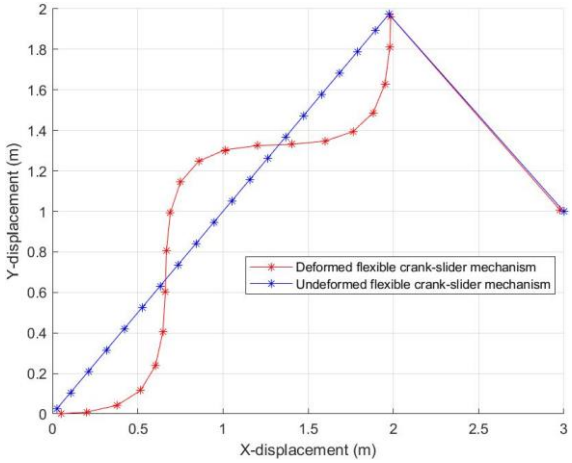

Mode 4 at 6.83Hz

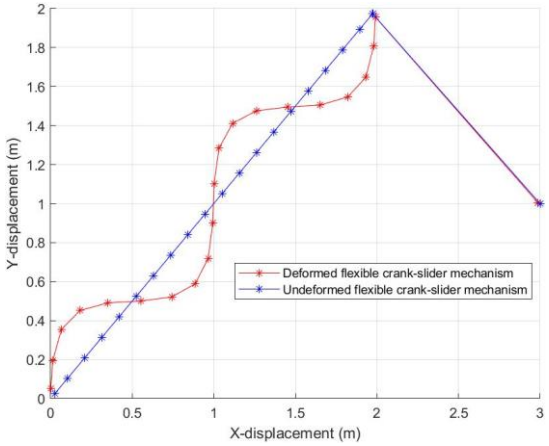

Mode 5 at 12.1Hz

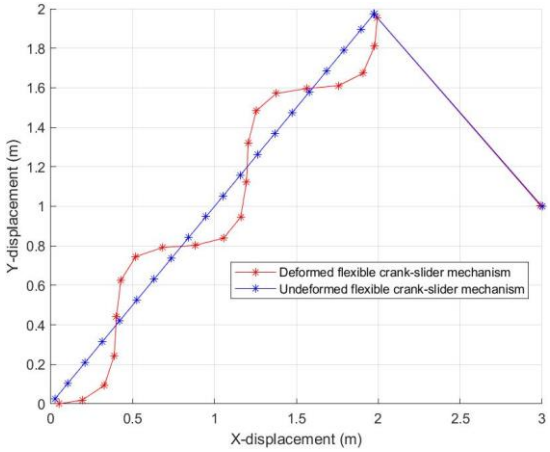

Mode 6 at 18.8Hz

Fig. 12: Mode 1 to 6 frequencies and shapes numerically predicted from the U-K formulated flexible crank-slider mechanism model

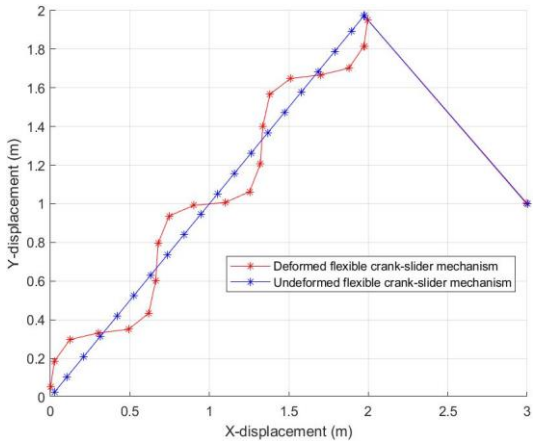

Mode 7 at 27.1Hz

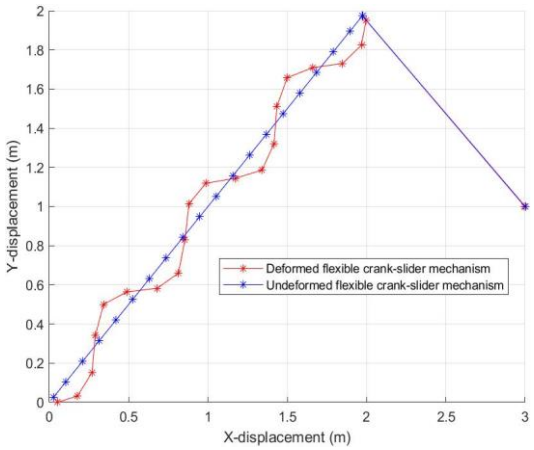

Mode 8 at 36.8Hz

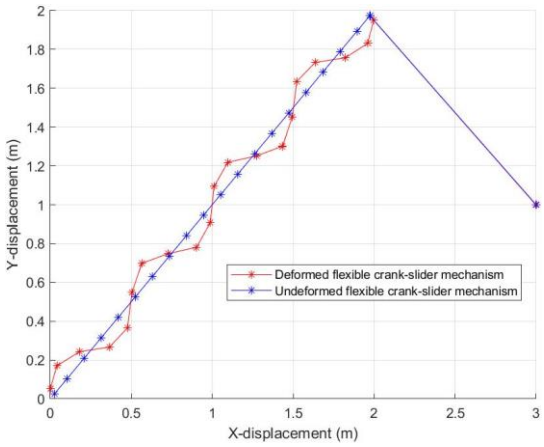

Mode 9 at 48.0Hz

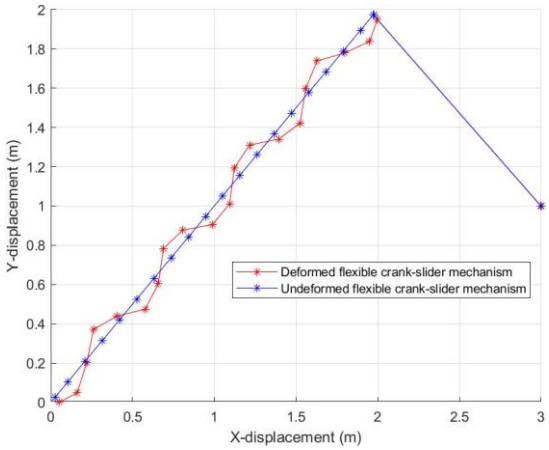

Mode 10 at 60.6Hz

Fig. 13: Mode 7 to 10 frequencies and shapes numerically predicted from the U-K formulated flexible crank-slider mechanism model

Throughout the plots in Figs. 12 and 13, what is referred to as deformed is the shape of the mechanism at its predicted modal frequency whilst undeformed refers to the initial configuration of the mechanism, with the crank link orientated at 45° from the horizontal. The U-K and Simscape model frequencies show a direct match, further validating the flexible crank-slider mechanism's modelling within the U-K formulation and the method of evaluating a linearised system's Jacobian matrix to extract its dynamic properties.

The mechanism's rigid modal frequency of 0.616Hz can be reobtained from the U-K flexible crank-slider mechanism model if the torsional spring stiffnesses within the crank link lumped parameter model are uniformly scaled from their default value of 34.806Nmrad^{-1} by a factor of 266, effectively stiffening the crank link as shown in Table. 6 and visualised in Fig. 14.

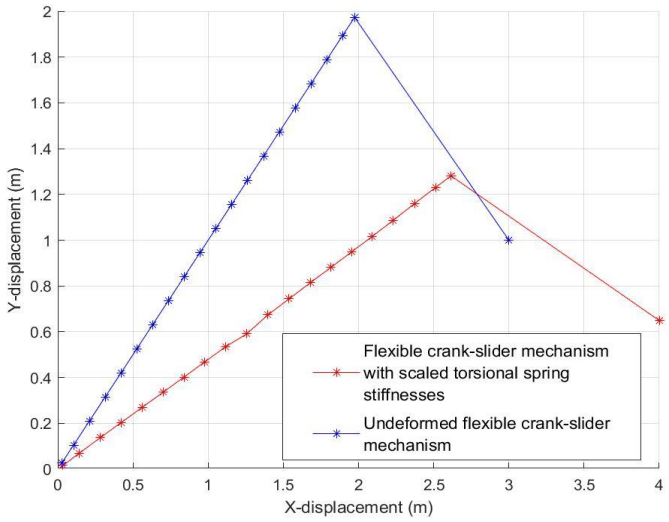

Fig. 14: Mode 1 of the flexible crank-slider mechanism with torsional spring stiffnesses scaled by a factor of 266x

Fig. 14 shows the U-K formulated mechanism model's numerically evaluated mode shape in regards to the X-Y displacement of the crank-slider mechanism's rigid element CGs including that for the rigid slider link. The 266x scaling factor was obtained by successively scaling the U-K mechanism model's crank link default torsional spring stiffness's uniformly until convergence is achieved with the 0.616Hz previously identified rigid modal frequency. The 266x torsional spring stiffness scaling factor resulted in a 0.601Hz rigid modal frequency for the Simscape mechanism model, constituting a 2.4% difference relative to the U-K model's 0.616Hz rigid modal frequency. Whilst this difference may be attributed to differences between the U-K and Simscape mechanism model formulations in addition to differences in methods to numerically extract the mechanism natural frequencies, this observation also highlights the sensitivity of the torsional spring stiffness parameter within the two mechanism models.

Fig. 14 highlights the effective rigid nature of the crank link at mode 1 due to the linear trend in rigid element CG translation points. Referring to Eq. (18), the 266x spring stiffness scaling factor physically translates to a corresponding scaling of either the crank link's second moment of area and subsequent cross sectional area, or Young's modulus of the crank link material along its entire length. To shed insight into how the evolution of the crank link flexibility influences the resulting mechanism's natural frequencies, the spring stiffness scaling factor is now gradually reduced and resulting mechanism's first 5 modal frequencies presented in Table. 6.

Table. 6: Influence of crank link torsional spring stiffness scaling factor on U-K crank-slider mechanism model natural frequencies.

	Torsional spring stiffness scaling factor				
Mode No.	**266.25x**	**200x**	**100x**	**50x**	**1x (original)**
1	0.616 Hz (Rigid mode frequency)	0.614 Hz	0.6101 Hz	0.600 Hz	0.285 Hz
2	13.2 Hz	11.4 Hz	8.13 Hz	5.83 Hz	1.73 Hz
3	49.9 Hz	43.3 Hz	30.6 Hz	21.6 Hz	3.06 Hz
4	111 Hz	96.4 Hz	68.2 Hz	48.2 Hz	6.83 Hz
5	197 Hz	171 Hz	121 Hz	85.4 Hz	12.1 Hz

The appearance of an asymptotic trend in the mechanism's first modal frequency in Table. 6 suggests any further stiffening and increase in spring stiffness scaling beyond a factor of 266x would most likely continue to yield a modal frequency that tends towards the limit of 0.62Hz. The influence of scaling the torsional spring stiffnesses on the crank-slider mechanism's resulting natural frequencies was also explored - the stiffening efficiency of the torsional springs for the first five modes were measured; the extent to which the mechanism's natural frequencies are influenced by stiffening the torsional springs within the mechanism's crank link lumped parameter model.

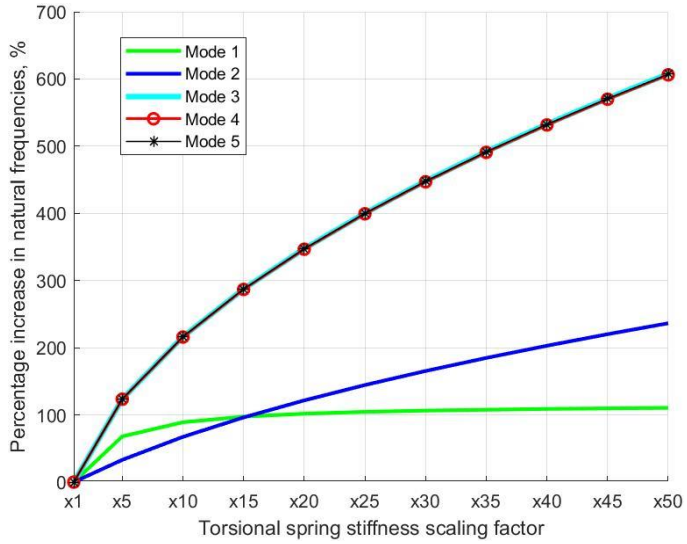

Fig. 15: Torsional spring stiffening efficiency

The results from Fig. 15 support the earlier view of an asymptotic limit in the mechanism's first modal frequency; stiffening the torsional springs in the crank link beyond a scaling factor of 15x appears to mark the onset of the frequency asymptotic limit. The findings also provide physical insight into the influence of the crank link's flexibility on specific modal frequencies. For example, if it is desired to redesign the original flexible crank-slider mechanism in order to shift its mode 1 frequency substantially beyond its rigid modal frequency of 0.616Hz, results from Table. 6 and Fig. 15 suggest avoid resorting

to stiffening the mechanism's flexible crank link as means to achieve this due to the diminishing returns and the asymptotic limitations associated with this particular modal frequency.

6. Conclusion

In this paper, the authors offer an alternative methodology to model flexible multibody systems using the Udwadia-Kalaba framework by extending the notion of rigid body modelling through a lumped parameter approach. In the lumped parameter approach used in this work, a flexible body is discretised into a series of rigid elements connected by torsional springs to represent bending flexibility. A mechanical system can be discretised into rigid elements and adapted within the U-K formulation; this was viewed as a benefit for incorporating a lumped parameter approach within the U-K formulation to model flexible multibody systems. An additional benefit is that within the U-K formulation, the ability to generalise beam model equations enables a U-K formulated beam model to be automatically formulated for a chosen number of rigid elements; the fidelity that a flexible beam is discretised into may be autonomously prescribed to facilitate the rapid dynamic analysis of flexible systems to meet accuracy requirements.

The Udwadia-Kalaba (U-K) modelling approach was shown to be applicable for modelling the dynamics of nonlinear and generic multibody systems under the influence of kinematical constraints. Initially, a flexible beam in the absence of boundary conditions was used to outline the process of discretising a flexible structure into lumped parameters within the U-K framework to capture the dynamics of flexibility. The resulting lumped parameters obtained within the U-K model were then validated against theoretically derived values.

A case study of a flexible crank-slider mechanism was presented to demonstrate the proof of concept of using a lumped parameter approach within the U-K framework to model flexible bodies integrated within wider mechanisms to capture flexible modes of the complete multibody system. The flexible crank-slider mechanism U-K model was validated through time history simulations against an alternatively formulated model and natural frequencies and mode shapes numerically obtained and validated.

By scaling the torsional spring stiffnesses within the flexible crank link, the influence on the resulting mechanism's natural frequencies were investigated, providing physical insight into the original system. On a wider scope, the implication is that modelling flexible multibody systems using the proposed U-K lumped parameter approach offers the ability to gain parametric insight into flexible multibody systems for their design. The prominence and potential of extending the application of the Udwadia-Kalaba formulations to model flexible multibody systems using a lumped parameter approach was shown in this study and advantages of adopting such an approach highlighted. Future research directions in this field include consideration of the application of modelling of flexible 3-D mechanical systems, which will introduce an additional layer of complexity in both the modelling and the interpretation of the dynamics.

Acknowledgments

The research presented is funded by EPSRC and BAE Systems through an Industrial CASE award (no. 17000065)

This research was funded in whole or in part by EPSRC and BAE Systems under Industrial CASE award no. 17000065. For the purpose of open access, the author has applied a 'Creative Commons Attribution (CC BY) public copyright licence to any Author Accepted Manuscript (AAM) version arising from this submission.

Nomenclature

$\mathbf{a}$	= Unconstrained acceleration vector
$\boldsymbol{A}$	= Matrix associated with the system's state accelerations
$\boldsymbol{b}$	= Vector of terms unassociated with the state accelerations of the system
CG	= Centre of gravity
E	= Young's Modulus
FE	= Finite element
I	= Second moment of area
g	= Gravitational acceleration
K_{T_i}	= i^{th} torsional spring stiffness
L	= Lagrangian quantity
l	= Length between centre of gravity of adjacent rigid elements
NF	= Natural Frequency
$\boldsymbol{M}$	= Mass matrix of the system
MBD	= Multi-Body Dynamic
ODEs	= Ordinary Differential Equations
Q_j	= Generalised force acting on the system associated with the j^{th} generalised coordinate.
q_j	= j^{th} generalised coordinate
R_D	= Energy function term due to the presence of dissipative forces
U-K	= Udwadia- Kalaba
(X,Y,θ)	= Global coordinate system
$\ddot{\mathbf{x}}$	= Vector of true accelerations of the multibody system including the influence of applied constraints
$+$	= Moore-Penrose generalised inverse

References:

[1]: Howell, L.L, Magleby, S.P, Olsen, B.M, *Handbook of Compliant Mechanisms*, John Wiley & Sons Ltd: Sussex, 2013,

[2]: Adams, The Multibody Dynamics Simulation Solution, https://www.mscsoftware.com/product/adams [retrieved 10 March 2021]

[3] DymoreSolutions, http://www.dymoresolutions.com [retrieved 10 March 2021]

[4] Ansys, Engineering Simulation Software, https://www.ansys.com/en-gb [retrieved in 2021]

[5] Udwadia, F.E and Kalaba, R.E, *Analytical Dynamics A New Approach*, Cambridge University Press: Cambridge,1996.

[6] Nielsen, M.C., Eidsvik, O.A., Blanke, M., Schjølberg, I., "Validation of Multi-Body Modelling Methodology for Reconfigurable Underwater Robots," Presented in the *OCEANS 2016 MTS/IEEE Monterey conference*, IEEE, Sept, 2016.

[7] Li, C., Zhao, H., Zhen, S., Sun, H., Shao, K., "Udwadia Kalaba theory for the control of bulldozer link lever," *Advances in Mechanical Engineering*, vol. 10, iss. 6, 2018

[8] Y. Xu, R. Liu, *Dynamic modeling of SCARA robot based on Udwadia-Kalaba theory*, Advances in Mechanical Engineering, Vol. 9(10), pp1-12, 2017

[9] Udwadia, F.E, Phohomsiri, P, "Explicit Poincaré equations of motion for general constrained systems. Part I. Analytical results"*Proceedings of the Royal Society A: Mathematical, Physical and Engineering Sciences*, Vol. 463, 2007

[10] Udwadia, F.E, Kalaba, R.R, "Explicit Equations of Motion for Mechanical Systems With Nonideal Constraints", ASME, Vol. 68, 2001

[11] Udwadia, F.E, Phohomsiri, P, "Explicit equations of motion for constrained mechanical systems with singular mass matrices and applications to multi-body dynamics", *Proceedings of the Royal Society*, Vol. 462, 2006

[12] Udwadia, F.E, Schutte, A.D, "Equations of motion for general constrained systems in Lagrangian mechanics". Acta Mechanica, Springer Verlag, 2010, 213 (102), pp.111-129.

[13] Bauchau, O.A, *Flexible Multibody Dynamics*, Springer, 2011

[14] Yap, E.J.H., Rezgui, D., Lowenberg, M.H., Neild, S.A. & Rahman, K., "Resonant Frequency Tuning of a Nonlinear Helicopter Inceptor Model: A Sensitivity Analysis,". in: *Proceedings of the 45th European Rotorcraft Forum*., Warsaw, Poland, pp. 1-14, 2019

[15] Simscape documentation, MathWorks ver. 2020b, https://uk.mathworks.com/products/simscape.html, [retrieved 10 March 2021]

[16] Antunes, J, Debut, V, *Development of a modal Udwadia-Kalaba formulation for guitar modelling*, International Symposium on Musical and Room Acoustics, 2016

[17] Antunes, J, Debut, V, *Dynamical computation of constrained flexible systems using a modal Udwadia-Kalaba formulation: Application to musical instruments*, The Journal of the Acoustical Society of America 141, 2017

[18] Antunes, J, Debut, V, Borsoi, L, Delaune, X, Piteau, P, *A modal Udwadia-Kalaba formulation for vibro-impact modelling of continuous flexible systems with intermittent contacts*, X International Conference on Structural Dynamics, EURODYN 2017

[19] Gutiérrez. J. L. R, Heidecker, A, *Nonlinear Controller Design for a Flexible Spacecraft*, The Journal of the Astronautical Sciences (2020) 67:1500–1520

[20] Pennestri, E, Valentini, P.P, de Falco, D, *An application of the Udwadia-Kalaba dynamic formulation to flexible multibody systems*, Journal of the Franklin Institute 347, 173-194, 2009.

[21] Géradin, M, Cardona, A, *Flexible Multibody Dynamics A Finite Element Approach*, Wiley, 2001

[22] Yap, E. J. H., Rezgui, D., Lowenberg , M. H., Neild, S. A., & Rahman,K. (2021). Towards development of a nonlinear and flexible multi-body helicopter inceptor model: a resonant frequency tuning study. In American Institute of Aeronautics and Astronautics (pp. 1-23)

[23] Patran, Complete FEA Modeling Solution, https://www.mscsoftware.com/product/patran [retrieved 10 March 2021]

[24] Neild, S.A, McFadden, P.D, Williams, M.S, *A Discrete Model Of A Vibrating Beam Using A Time-Stepping Approach*, Journal of Sound and Vibration (2001) 239(1), 99-121

[25] Moore-Penrose pseudoinverse documentation, MathWorks, https://www.mathworks.com/help/matlab/ref/pinv.html, [retrieved 10 March 2021]

[26] How Simscape Simulation Works documentation, https://www.mathworks.com/help/physmod/simscape/ug/how-simscape-simulation-works.html, [retrieved 25 May 2021]